Available online at www.sciencedirect.com
SCIENCE DIRECT®
ELSEVIER
Journal of Nuclear Materials 322 (2003) 235–241
journal of nuclear materials
www.elsevier.com/locate/jnucmat

Diffusion bonding of titanium to 304 stainless steel

M. Ghosh [a], K. Bhanumurthy [b], G.B. Kale [b,*], J. Krishnan [c], S. Chatterjee [a]

[a] Department of Metallurgy, Bengal Engineering College (a Deemed University), Howrah 711103, WB, India
[b] Materials Science Division, Bhaba Atomic Research Centre, Trombay, Mumbai 400085, India
[c] CDM, Bhabha Atomic Research Centre, Trombay, Mumbai 400085, India

Received 16 September 2002; accepted 27 July 2003

Abstract

Diffusion bonding between commercially pure titanium and an austenitic stainless steel (AISI 304) has been carried out in the temperature range of 850–950 °C for 2 h at uniaxial pressure of 3 MPa in vacuum. The microstructure of the diffusion zone has been analysed by optical and scanning electron microscopy (SEM). The interdiffusion of the diffusing species across the interface has been evaluated by electron probe microanalysis (EPMA). The reaction products formed at the interface have been identified by X-ray diffraction technique. It has been observed that the diffusion zone is dominated by the presence of the σ phase close to the stainless steel side and the solid solution of β-Ti (solutes are Fe, Cr and Ni) close to the titanium. The presence of Fe_2Ti and FeTi has been found in the reaction zone. It has been observed that the bond strength (~222 MPa) is highest for the couple processed at 850 °C and this value decreases with rise in joining temperature. The variation of strength of the transition joints is co-related with the microstructural characteristics of the diffusion zone.

1. Introduction

Diffusion bonding is an important fabrication technique for making components in electronic, nuclear and aerospace industries [1,2]. This technique provides novel joining operation for similar and dissimilar materials without gross microscopic distortion and with close dimensional tolerance. This method has already proved considerable potential for joining of Ti and Al base alloys [3–7]. Joining of varieties of dissimilar and similar materials has already been carried out by diffusion bonding, though many of the parameters of the thermomechanical processing are yet to be established on commercial scale [8–13]. The joints between Ti and stainless steel find wide applications in nuclear industry. The conventional fusion welding of these two materials results in segregation of chemical species, stress concentration sites and formation of intermetallics at interfaces as Ti and Fe are not completely soluble in solid state and form Fe_2Ti and FeTi intermetallic phases [14,15]. All these deleterious effects ultimately lead to premature failure of components in service condition. Extensive work has already been reported to produce diffusion bonded joints of commercially pure Ti (CP-Ti) to the austenitic stainless steel (SS) [16–18]. The earlier work on diffusion reaction between Ti/stainless steel indicated the formation of Fe, Cr and Ni based intermetallic compounds [15–19]. It is also suggested that the formation of intermetallic compounds is more significant for the diffusion couple annealed above 900 °C [16]. The TEM studies on Ti/316 stainless steels confirmed the formation of σ, Fe_2Ti, FeTi, Fe_2TiO_4, and TiC in the reaction zone [15]. The recent work on the diffusion reaction between Ti and stainless steel (AISI 304) at 800 °C for 96 h did not report the formation of any intermetallic compounds [20]. Most of the earlier studies are restricted to the characterisation of intermetallic compounds formed in the diffusion zone. To the best of the knowledge of the authors only data on mechanical strength of such bonds is by Kale et al. [19] and

* Corresponding author.
E-mail address: gbkale@apsara.barc.ernet.in (G.B. Kale).

0022-3115/$ - see front matter © 2003 Elsevier B.V. All rights reserved.
doi:10.1016/j.jnucmat.2003.07.004

Kato et al. [21]. The present paper aims in evaluating the mechanical strength at various bonding temperatures. The strength data has been rationalized on the basis of the microstructure of the diffusion zone.

2. Experimental

CP-Ti and 304SS used in the present investigation were in hot-rolled condition. Their chemical analysis and room temperature tensile properties are presented in Tables 1 and 2 respectively. In this investigation two types of geometries have been chosen namely (a) rectangular and (b) cylindrical type specimens for investigation. The rectangular type specimens of dimension $10\times10\times5$ mm are essentially used for detailed metallurgical analysis and cylindrical type samples of 15 mm diameter and 30 mm length have been used for mechanical testing. The mating surfaces of the rectangular and cylindrical specimens have been metallographically polished to a 1 μm diamond finish, cleaned in acetone to remove adhered contaminants and dried in air and have been bonded as mentioned below.

The diffusion bonding set up was designed and developed indigenously and consisted of 5000 N load cell, Inconel plunger for transferring load to sample, Inconel sample supporting die, stainless steel (SS) frame with top and intermediate guide plate. A split type cylindrical furnace with a maximum operating temperature of 1000 °C and constant temperature zone of 50 mm was used for bonding the specimens. The chromel–alumel thermocouple was inserted for measuring temperature and was placed close to the bond line. The set up was kept in a vacuum chamber, operated by a vapour diffusion pump coupled with a single stage rotary pump. The polished mating faces of Ti and SS have been kept in contact and loaded in the diffusion bonding set up. The entire assembly was placed in a vacuum chamber and 10^{-4} mbar vacuum has been maintained through out the bonding cycle. The couples have been diffusion bonded at 850, 900 and 950 °C for 2 h under uniaxial pressure of 3 MPa. Heating rate for the bonding cycle was 14 °C/min and after bonding the whole assembly was cooled in vacuum chamber.

The rectangular diffusion couples thus prepared were cut off perpendicularly from the joint portion and metallographically polished to 1 μm diamond finish. Microstructural features were examined by optical microscope (Correct SDME TR5). The concentration profiles were determined by electron probe microanalyser (CAMECA SX 100) operating at 15 kV with a stabilized beam current of 40 nA. A LiF crystal was employed to diffract TiK_α, FeK_α, CrK_α, NiK_α X-ray lines. The reaction products formed at the joint portion of diffusion bonded couple were characterised by X-ray diffractometer (Philips PW 1830) at an operating voltage of 30 kV and current of 20 mA. Copper target was used and scanning span was 20–70° with a step of 0.02° $(=2\theta)$/s. The room temperature tensile strength of the cylindrical transition joints were evaluated (INSTRON 4204) at a cross-head speed of 0.00083 mm/s, using cylindrical test pieces with a diameter of 4 mm and gauge length of 20 mm, machined from diffusion couples with the bonded interface at the centre of the gauge length.

3. Results and discussion

3.1. Microstructural characterisation of the diffusion zone

The optical micrographs for the bonded specimen at 850, 900 and 950 °C for 2 h are shown in Fig. 1. The micrographs exhibit a good bonding along the interface of the bonded couples and the interface is free from discontinuities and microcracks. Four distinct regions are observed on the micrographs corresponding to (a) parent stainless steel with annealing twins (b) heavily etched band, presumably intermetallic compounds (c) retained β-Ti solid solution containing Fe, Cr and Ni and (d) parent Ti with fine α-needles. These micrographs

Table 1
Chemical composition of the base materials (elements in wt%)

Alloy	C	Fe	Ti	Mn	Si	P	S	Cr	Ni	Mo	Cu
CP-Ti	0.02	0.10	Bal	–	–	–	–	–	–	–	–
304 SS	0.01	Bal	–	1.15	0.23	0.028	0.012	18.9	11.45	0.03	0.08

Table 2
Room temperature tensile properties of the base metals

Alloy	0.2% proof stress (MPa)	Ultimate tensile strength (MPa)	Percentage of fracture elongation
CP-Ti	204.60	318.60	22.8
304 SS	131.50	568.60	46.6

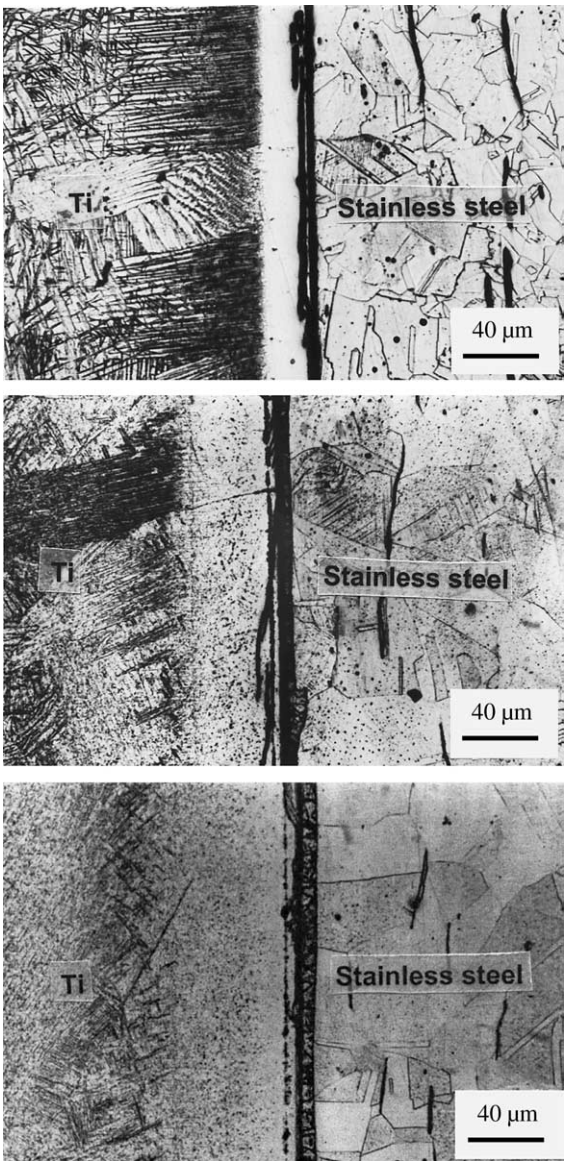

Fig. 1. Optical micrographs of the Ti/stainless steel diffusion couples bonded at (a) 850 °C (above), (b) 900 °C (middle) and (c) 950 °C (bottom) for 2 h.

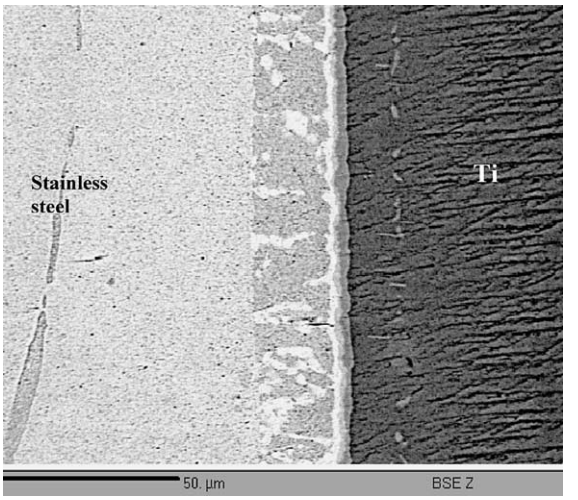

Fig. 2. Back-scattered electron image (BSE) for the specimen bonded at 950 °C for 2 h in un-etched condition.

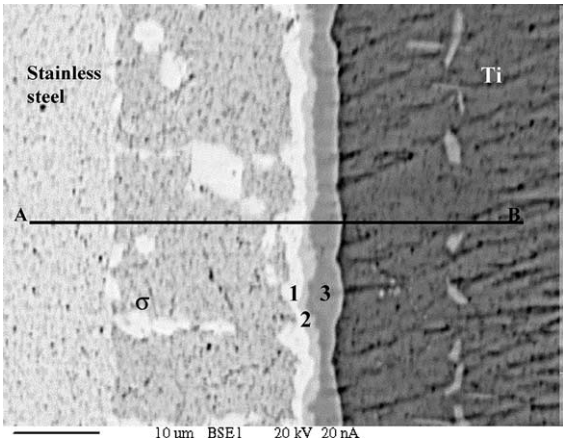

Fig. 3. BSE image taken at higher magnification (region corresponding to Fig. 2) for the specimen bonded at 950 °C for 2 h in un-etched condition.

clearly indicate that there is substantial increase in the width of diffusion zone with increase in bonding temperature.

Back-scattered electron image (BSE) for the specimen bonded at 950 °C for 2 h in un-etched condition is shown in Fig. 2 and corresponding figure taken at higher magnification is given in Fig. 3. The micrograph clearly indicates formation of several layers in the diffusion zone and these features could not be resolved in optical micrographs. Concentration profiles for the specimen bonded at 850 and 950 °C for 2 h are exhibited in Figs. 4 and 5 respectively. In addition, concentration profiles of Fe, Cr, Ni and Ti across the region A–B (marked on Fig. 3) are illustrated in Fig. 6. In fact, several points have been chosen in each phase with a counting time of minimum 100 s for better statistics and the average corrected composition of each phase is plotted in Fig. 6. The BSE for the couple bonded at 950 °C (Fig. 3) clearly shows the formation of σ phase near the stainless steel. The average composition of this σ phase is Fe∼59.8–61.8 at.%, Cr∼29.2–31.8 at.%, Ni∼4.7–5.8 at.% and Ti (balance) and the width of this is about 20 μm. It is also noteworthy that composition of this phase does not change significantly with the increase in bonding

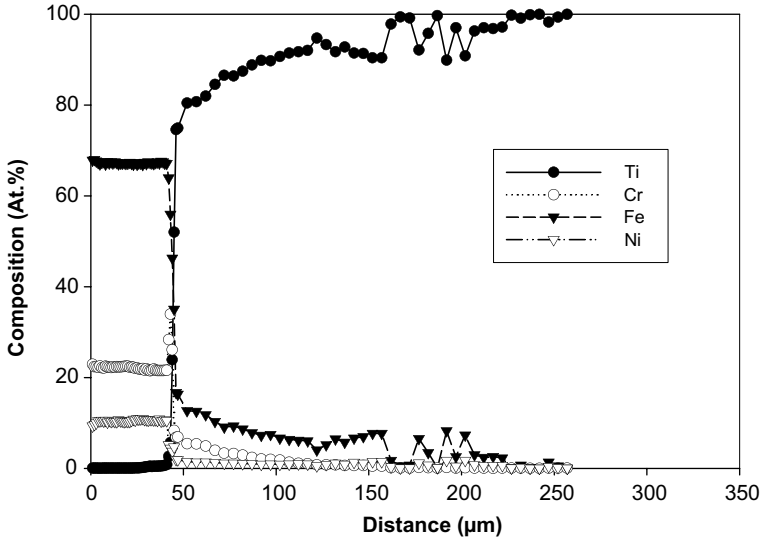

Fig. 4. Concentration profile of Fe, Cr, Ni and Ti for the specimen bonded at 850 °C for 2 h.

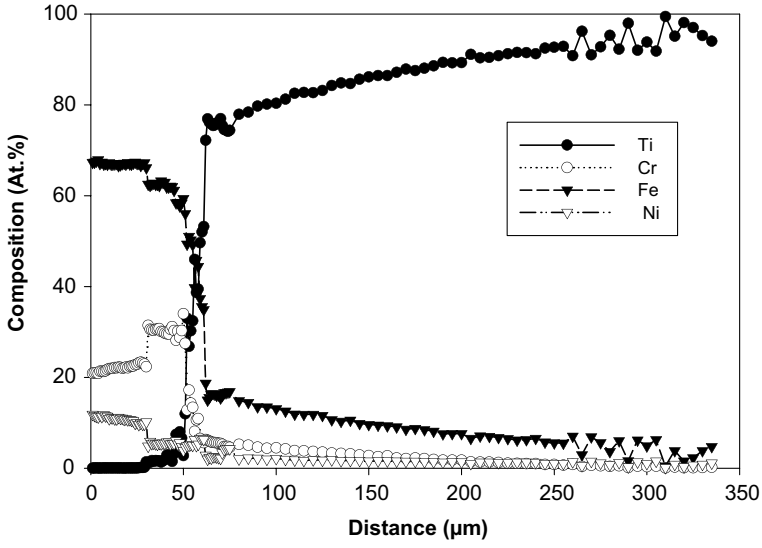

Fig. 5. Concentration profile of Fe, Cr, Ni and Ti for the specimen bonded at 950 °C for 2 h.

temperature. The concentration profiles suggest that Fe and Ni diffuse in Ti to large extent as compared Cr. Immobility of Cr might have lead to the formation of σ phase. The back scattered image exhibits dispersion of precipitates having composition Ni∼5.67 at.%, Cr∼30.59 at.%, Fe∼62.61 at.% and balance Ti within this σ phase and perhaps this intermetallic is χ phase [15]. The formation of σ phase was also confirmed by X-ray diffraction studies on the fracture surface of the stainless steel side. However the presence of χ phase could not been confirmed by X-ray diffraction possibly due to its small volume fraction in the reaction zone. The formation of the χ phase was also reported based on the TEM studies on Ti(6242)/316 stainless steel diffusion couples annealed at 900 °C for 0.5 h [15].

The phase adjacent to σ phase is Fe_2Ti(Cr, Ni) intermetallic (marked as 1 in Fig. 3) and this phase contains substantial amount of Cr (∼24.8 at.%), Ni (∼4.8 at.%). Adjacent to the Fe_2Ti(Cr, Ni) phase a narrow phase of thickness, 1–2 μm could be noticed (marked as

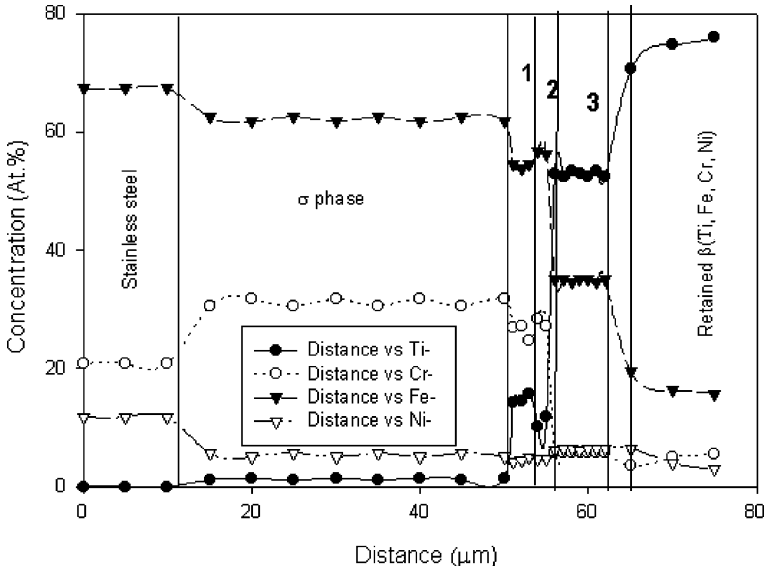

Fig. 6. Concentration profiles of Fe, Cr, Ni and Ti across the region A–B (marked on Fig. 3).

2 in Fig. 3), and the approximate composition of this phase is Cr (~30.0 at.%), Fe (~56.0 at.%), Ni (~4.0 at.%) and the balance is Ti. The composition of this phase could not be unambiguously resolved by EPMA due to its small thickness. This phase could be a mixture of $TiCr_2 + Fe_2Ti(Cr)$ and this two phase field has been reported in the Fe–Ti–Cr ternary isotherm at 900 °C [22]. Adjacent to $TiCr_2$+$Fe_2Ti(Cr)$ phase is clearly Fe-Ti(Cr, Ni) intermetallic phase (marked as 3 in Fig. 3) with Fe (~35.2 at.%), Cr (~5.8 at.%), Ni (~6.4 at.%) and balance Ti. The presence of Fe_2Ti (Cr) and FeTi(Cr) have been also confirmed by X-ray diffraction studies. Next to FeTi intermetallic phase is solid solution phase of β-Ti with considerable amount of Fe, Cr and Ni dissolved in it. Fine dispersion of precipitates which are situated parallel to the diffusion zone have been also identified within β-Ti and perhaps they are Fe_2TiO_4. These oxides might have formed in the initial stages of the diffusion couple formation and have migrated towards to Ti side. Faster diffusion of β-Ti in stainless steel and formation of Kirkendall pores has been discussed extensively in the literature [15].

The recent study by He et al. [23] on the diffusion studies between Ti alloys to stainless steel mesh at 900 °C reported the formation of Ti_2Fe, TiFe adjacent to the titanium alloys and intermetallic compounds $TiFe_2$, σ-Fe–Cr phase adjacent to stainless steel. The TEM/SEM investigation on interdiffusion studies between stainless steel (AISI 316) and commercially pure titanium [15] also showed the formation of TiFe, $TiFe_2$, σ-Fe–Cr and do not indicate the formation of Ti_2Fe. In fact, Ti_2Fe phase is not an equilibrium phase reported in the binary Ti–Fe phase diagram [24]. The present experiments confirmed the formation of σ phase close to the stainless steel and $Fe_2Ti(Cr,Ni)$, $Cr_2Ti(Fe)$, FeTi(Cr,Ni) and β-Ti(Fe,Cr,Ni) solid solution close to the titanium side of the diffusion couple. Based on the details of the formation of various phases, a diffusion path for the diffusion couple annealed at 950 °C is stainless steel/σ phase with χ phase (particles)/$Fe_2Ti(Cr,Ni)$/$Fe_2Ti(Cr,Ni)$ + $Cr_2Ti(Fe)$/FeTi(Cr,Ni)/β-Ti(Fe,Cr,Ni)/Ti. Assuming that the interaction of Ni is negligible in this reaction, the observed diffusion path is consistent with the reported Fe–Cr–Ti ternary isotherm at 950 °C [22].

3.2. Temperature dependence of layer growth

The temperature dependence of the individual phase width (X) (Table 3) can be represented assuming the growth of each phase to be parabolic by equation

$$X = K_0 t^{1/n} \exp(-Q_p/RT), \quad (1)$$

where $K = K_0 \exp(-Q_p/RT)$ m/s$^{1/2}$, inter-diffusion rate constant, t time of diffusion annealing in seconds, Q_p activation energy for layer growth in kJ/mol, and $n = 2$

Table 3
Layer growth kinetics of the intermediate phases formed in the diffusion zone

Intermetallic phases	Activation energy Q (kJ/mol)	K_0 (m/s$^{1/2}$)
σ	184.3	18.7
Fe_2Ti	125.8	8.7×10^{-3}
FeTi	124.9	1.4×10^{-2}

is assumed for the parabolic growth of the individual phases.

Based on the linear plot of $\ln X$ vs. $1/T$ the values of Q_p and K_0 are estimated for the σ, Fe_2Ti and FeTi phases and the same are listed in Table 3. The activation energy values calculated taking into the overall thickness for the Ti/stainless steel (304) system in the temperature range 750–859 °C is reported as 73.96 kJ/mol [20]. The values of the activation energies evaluated in the present studies are generally higher compared to the values reported earlier [20]. This large difference could be due to the total absence of any intermetallic compounds in the diffusion zone for all the couples annealed in the temperature range 700–850 °C in the earlier studies [20] compared to the formation of the σ, Fe_2Ti and FeTi phases in the present studies.

3.3. Mechanical properties of the bonded specimens

The bond strength and the % of elongation obtained in the present studies are listed in Table 4. A highest strength value of ~222 MPa with adequate ductility (~9%) was obtained for the samples bonded at 850 °C and the bond strength decreases with increase in temperature. At bonding temperature of 850 °C, CP-Ti is in two phase field (hcp + bcc) and the combined width of the diffusion zone of the σ, Fe_2Ti and FeTi phases is about 7 μm. At the intermediate bonding temperature i.e. 900 °C, CP-Ti is in lower part of the β phase field and at 950 °C is in complete β-phase field. High bonding temperature results in profuse diffusion of chemical species and the combined width of the diffusion zone of the σ, Fe_2Ti and FeTi phases is about 30 μm for the specimen bonded at 950 °C. The formation of intermetallics and segregated layers in the couples at higher temperatures couples with excessive grain growth are mainly responsible for lowering the strength value and reduction in the ductility. In a similar system, Kato et al. achieved 60% bond strength of Ti along with <2.2% ductility [21] and Kale et al. specified, bond strength of 150 MPa [19]. Present experiments showed a substantial increase in the strength values of about 70% of the parent Ti with a relative ductility of about 9%. This discrepancy in the strength values based on the present studies and those reported earlier could be due to variation in the applied pressure and subsequently large change in the contact area at the time of bonding. The tensile samples failed in the diffusion zone on the stainless steel side. The X-ray diffraction studies confirmed the presence of brittle σ phase at the fractured surface, which could be responsible for the failure.

Table 4
Room temperature tensile properties of diffusion bonded assemblies at different temperatures for 2 h

Assembly designation	Bonding temperature (°C)	UTS (MPa)	Percentage of elongation
DB-1	850	222.10 ± 9	9.1
DB-2	900	193.00 ± 6	3.9
DB-3	950	128.90 ± 4	2.1

4. Conclusions

- Diffusion bonding of CP-Ti to 304 SS has been achieved using indigenously designed and fabricated press. The micrographs clearly indicated excellent bonding at the interface and free from microcracks and discontinuities.
- The diffusion zone indicated the formation of σ, Fe_2Ti and FeTi phases in the diffusion zone and the activation energy values for these phases are found to be 184.3, 125.8 and 124.9 kJ/mol respectively. The diffusion path evaluated on the basis of the concentration profiles of the main diffusing elements could be correlated with the Fe–Cr–Ti ternary isotherm at 950 °C.
- Tensile testing of the diffusion bonded specimen at 850 °C indicated a bond strength ~222 MPa with adequate ductility of ~9%. The bond strength decreases with increase in the bonding temperature and this is essentially due to the increase in the width of the brittle intermetallic compounds.

Acknowledgements

The authors gratefully acknowledge the financial support rendered by Board of Research in Nuclear Science, Govt. of India for carrying out this research work. They are also grateful to Dr S. Banerjee, Director, Materials Group, BARC, Mumbai, India, Dr P.K. De, Head, Materials Science Division and Professor A. Sengupta, Vice Chancellor, B.E. College (a Deemed University), Howrah, India for their keen interest in this investigation.

References

[1] G. Cam, M. Kocak, Int. Mater. Rev. 43 (1998) 1.
[2] W.H. King, W.A. Owczarski, Weld. J. 46 (1981) 289S.
[3] M.T. Salehi, J. Pilling, N. Ridly, D.L. Hamilton, Mater. Sci. Eng. A 150 (1992) 1.
[4] Z.C. Wang, N. Ridley, G.W. Lorimer, D.K. Knuss, G.A.D. Briggs, J. Mater. Sci. 31 (1996) 5199.
[5] Y. Huang, F.G. Humphreys, N. Ridley, Z.C. Wang, Mater. Sci. Technol. 14 (1998) 405.
[6] D.V. Dunford, P.G. Partridge, Mater. Sci. Technol. 8 (1992) 385.
[7] J. Pilling, Mater. Sci. Eng. 100 (1988) 137.

[8] P.C. Tortorici, M.A. Dayananda, Scr. Metall. 38 (1998) 1863.
[9] A. Calvo, A. Urena, J.M.G. DeSalazor, F. Molleda, J. Criado, J. Mater. Sci. 23 (1988) 1231.
[10] J.G. Luo, V.L. Acoff, Weld. J. 18 (2000) 239S.
[11] A. Wishbey, P.G. Partridge, Mater. Sci. Technol. 9 (1993) 441.
[12] Y. Nakao, Y. Shinozaki, M. Hamada, ISIJ Int. 31 (1991) 1260.
[13] D.C. Eckman, B.Z. Rosenblum, C.Q. Bowles, J. Mater. Sci. 27 (1992) 49.
[14] P. He, J. Zhang, R. Zhou, X. Li, Mater. Charact. 43 (1999) 288.
[15] B. Aleman, I. Gutierrez, J.J. Urcola, Mater. Sci. Technol. 9 (1993) 633.
[16] K. Bhanumurty, G.B. Kale, J. Mater. Sci. Lett. 12 (1993) 1879.
[17] G.V.T. Ranzetta, J. Pearson, Met. Mater. A 13 (1969) 478.
[18] A. Changqing, J. Zangpeng, J. Less Common Mater. 162 (1990) 315.
[19] G.B. Kale, K. Bhanumurthy, Indian Institute of Welding (Mumbai) Int. Weld. Conf. (1994) 042.
[20] G.B. Kale, R.V. Patil, P.S. Gawde, J. Nucl. Mater. 257 (1998) 44.
[21] H. Kato, M. Shibata, K. Yoshikawa, Mater. Sci. Technol. 2 (1986) 405.
[22] P. Villars, 2121, in: A. Prince, H. Okamata (Eds.), Hand Book of Ternary Alloy Phase Diagrams Vol. 7, 1995, p. 8915/9162; Vol. 8, p. 10655, ASM, Metals Park, Ohio.
[23] P. He, J.-H. Zhang, X.-Q. Li, Mater. Sci. Technol. 17 (2001) 1158.
[24] T.B. Massalski (Ed.), Binary Alloy Phase Diagrams, 2nd Ed., ASM, Metals Park, Ohio, 1990.